Supplementary Information

Experimental section

Materials: $Co(NO_3)_2 \cdot 6H_2O$, NH_4F, Urea(CH_4N_2O), NH_4Cl, $N_2H_4 \cdot H_2O$, HNO_3, HCl, Na_2SO_4, NaOH, C_2H_5OH were purchased from Aladdin Ltd. (Shanghai, China). Sodium salicylic ($C_7H_5O_3Na$), p-dimethylaminobenzaldehyde ($C_9H_{11}NO$), sodium citrate dehydrate ($C_6H_5Na_3O_7 \cdot 2H_2O$), sodium nitroferricyanide dihydrate ($C_5FeN_6Na_2O \cdot 2H_2O$), sodium hypochlorite solution (NaClO) were purchased from Beijing Chemical Corp. (China). 117 Nafion membrane (Alfa Aesar), 5wt % Nafion (Dupont). All chemicals were used as received without further purification. Carbon cloth (CC) was Provided by Hongshan District, Wuhan Instrument Surgical Instruments business. And it was pretreated in HNO_3 and then cleaned by sonication in water and C2H5OH for several times to remove surface impurities. The water used throughout all experiments was purified through a Millipore system.

Preparation of *Co(OH)F/CC* : Co(OH)F/CC was prepared as follows. In a typical synthesis, $Co(NO_3)_2 \cdot 6H_2O$ (0.582 g), NH_4F (0.186 g) and urea (0.60 g) were dissolved in deionized water (40 mL) in a 50 mL beaker. After continuously stirring for 30 min, the solution was then transferred to a 50 mL Teflon-lined autoclave with a piece of CC (2 cm × 3 cm). The autoclave was heated to 120 °C, and kept at that temperature for 6 h. After cooling to room temperature, the resulting precipitates were washed several times with deionized water, and then dried at 60 °C for 6 h. Then the Co(OH)F/CC was obtained.

Preparation of *CoP_3/CC* : The synthesis method of CoP_3/CC is to take a small piece of 2 cm long and 1 cm wide precursor carbon cloth and 30 mg of red phosphorus into a small quartz tube and vacuum seal, then the small quartz tube is heated in a muffle furnace, with 650 °C for 5 h. Finally, the carbon cloth was taken out and washed with water and alcohol several times at room temperature for 10 h to obtain a CoP_3/CC (loading: 1.01 mg cm^{-2}).

Preparation of *CoP_2/CC* and *CoP/CC*: The synthesis scheme of CoP_2/CC and CoP/CC is the same as the synthesis scheme of CoP_3/CC. But the amount of red phosphorus is 2/3 and 1/3 respectively. Finally, CoP_2/CC (loading: 1.21 mg cm^{-2}) and

CoP/CC (loading: 1.32 mg cm^{-2}) materials can be obtained.

Characterization: The XRD patterns were obtained from a LabX XRD-6100 X-ray diffractometer with Cu Kα radiation (40 kV, 30 mA) of wavelength 0.154 nm (SHIMADZU, Japan). The X-ray photoelectron spectroscopy (XPS) measurements were performed on an ESCALABMK II X-ray photoelectron spectrometer using Mg as the exciting source. The scanning electron microscopy (SEM) measurements were carried out on a XL30 ESEM FEG scanning electron microscope at an accelerating voltage of 20 kV. Transmission electron microscopy (TEM) characterization was performed using a HITACHI H-8100 electron microscopy (Hitachi, Tokyo, Japan) operated at 200 kV. The UV-visible adsorption spectra were recorded on a spectrophotometer (Shimadazu, UV-1800).

Determination of NH_3: 4 mL of sample was removed from the cathodic chamber, then added into 50 μL of oxidizing solution containing NaClO (ρCl = 4~4.9) and NaOH (0.75 M), then added 500 μL coloring solution containing 0.4 M $C_7H_6O_3$ and 0.32 M NaOH and 50 μL catalyst solution (0.1 g $Na_2[Fe(CN)_5NO]\cdot 2H_2O$ diluted to 10 ml with deionized water) in turn. Absorbance measurements were performed after two hour at λ = 655 nm. Rate of NH_3 formation was calculated using the following equation:

$$R_{NH3}\ (\text{mol}\cdot\text{cm}^{-2}\cdot\text{s}^{-1}) = \frac{x\ (ppm)\ \times 10^{-3}(g/mg)\ \times V(L)}{Mr_{NH_4^+}(g/mol)\ \times t(s)\ \times S(cm^{-2})}$$

Where:

R_{NH3} (mol·cm^{-2}·s^{-1})：is ammonia formation rate in mol·cm^{-2}·s^{-1},

X (ppm): is ammonia concentration in the detection solution in ppm (mg/L),

V (L): is volume of solution in litter,

$Mr_{NH_4^+} = 18\ (g/mol)$,

t (s): is the reaction time in seconds,

S: is active area of the membrane electrode in cm^2.

Determination of FE: Assuming 3 electrons were needed to produce one NH_3 molecule, the FE in 0.1 M Na_2SO_4 could be calculated as follows:

$$FE_{NH3}(\%) = \frac{3 \times R_{NH3}(mol \cdot cm^{-2} \cdot s^{-1}) \times t(s) \times S(cm^{-2}) \times F}{I(A) \times t(s)}$$

where:

F is the Faraday constant,

I(A): the average of current during the reaction.

Electrochemical measurement: Electrochemical measurements were performed with a CHI660E electrochemical analyzer (CH Instruments, Inc.) in a standard three-electrode setup, with the use of CoP_3/CC as the working electrode, a graphite rod as the counter electrode and a saturated Ag/AgCl electrode as the reference electrode. The reaction cell was separated by Nafion 117 membrane. Polarization curves were obtained using linear sweep voltammetry with a scan rate of 5 mV s^{-1} and were the steady-state ones after several cycles. In all measurements, saturated Ag/AgCl electrode was calibrated with respect to RHE as following: in 0.1 M Na_2SO_4 aqueous solution, E(RHE) = E(Ag/AgCl) + 0.059 × pH + 0.197 V. All experiments were carried out at room temperature (~ 25 °C). The presented current density referred to the geometrical area of the Carbon cloth. For N_2 reduction experiments, the electrolyte was purged with N_2 for 30 min before the measurement. Pure N_2 was continuously fed into the cathodic compartment with a flow rate of 10 cm^3 min^{-1} during the experiments.

DFT methods: The present first principle calculations are performed with the projector augmented wave (PAW) method based on DFT. The exchange-functional is treated using the generalized gradient approximation (GGA) of Perdew-Burke-Ernzerhof (PBE) functional. The cut-off energy of the plane-wave basis is set at 400 eV for optimize calculations of atoms optimization. The vacuum spacing in a direction perpendicular to the plane of the catalyst is at least 10 Å. The Brillouin zone integration is performed using 3 × 3 × 1 Monkhorst and Pack k-point sampling for interface. The self-consistent calculations apply a convergence energy threshold of 10^{-6} eV. The maximum Hellmann-Feynman force for each ionic optimization step is 0.05 eV/Å. In addition, spin polarizations is also considered in all calculations. Finally, the free energies are obtained by G=Etotal+EZPE-TS, where Etotal, EZPE, and TS are the ground-state energy, zero-point energies, and entropy terms, respectively. In our

calculation, the bottom layers (three layers) were kept fixed at their bulk position. The vibrational frequencies and entropies of molecules in the gas phase were taken from the NIST database.

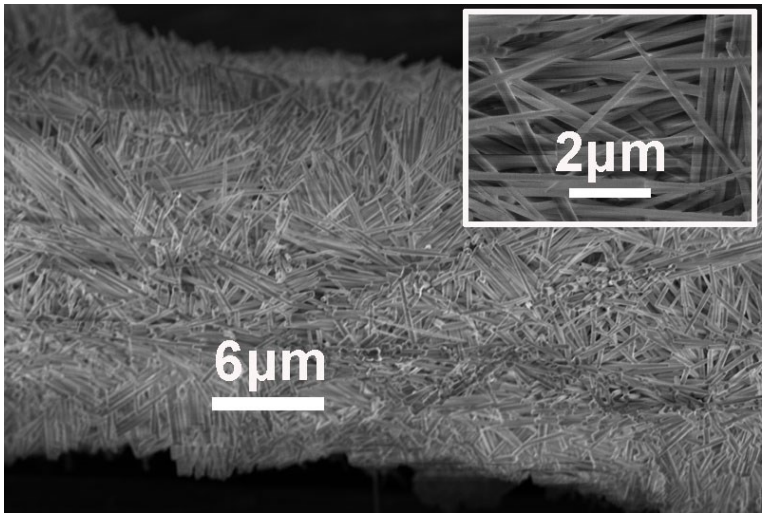

Fig. S1. SEM images of hydroxide precursor.

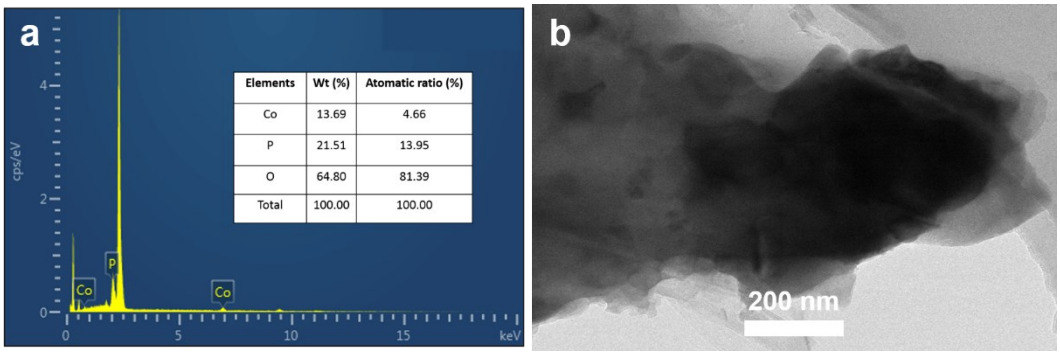

Fig. S2. (a) EDX spectrum of CoP_3. (b) TEM image of a single CoP_3 nanoneed.

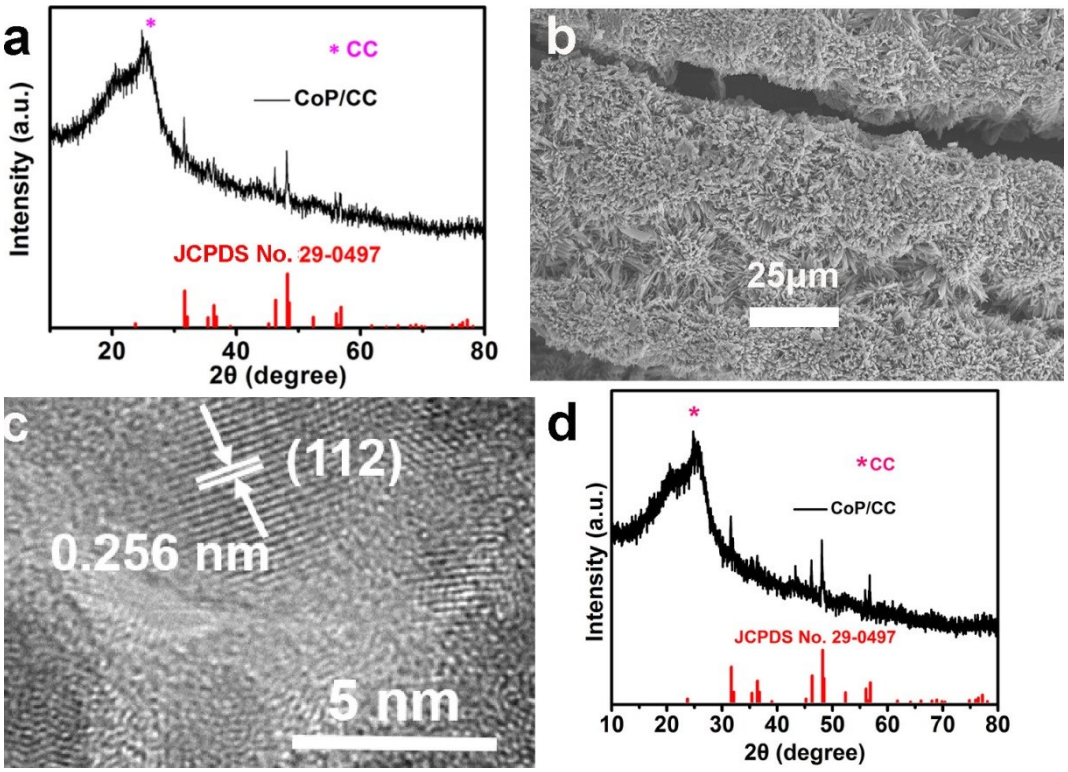

Fig. S3. (a) XRD pattern for CoP/CC. (b) SEM image for CoP/CC. (c) HRTEM image for CoP. (d) XRD pattern for CoP/CC after long-term NRR electrolysis.

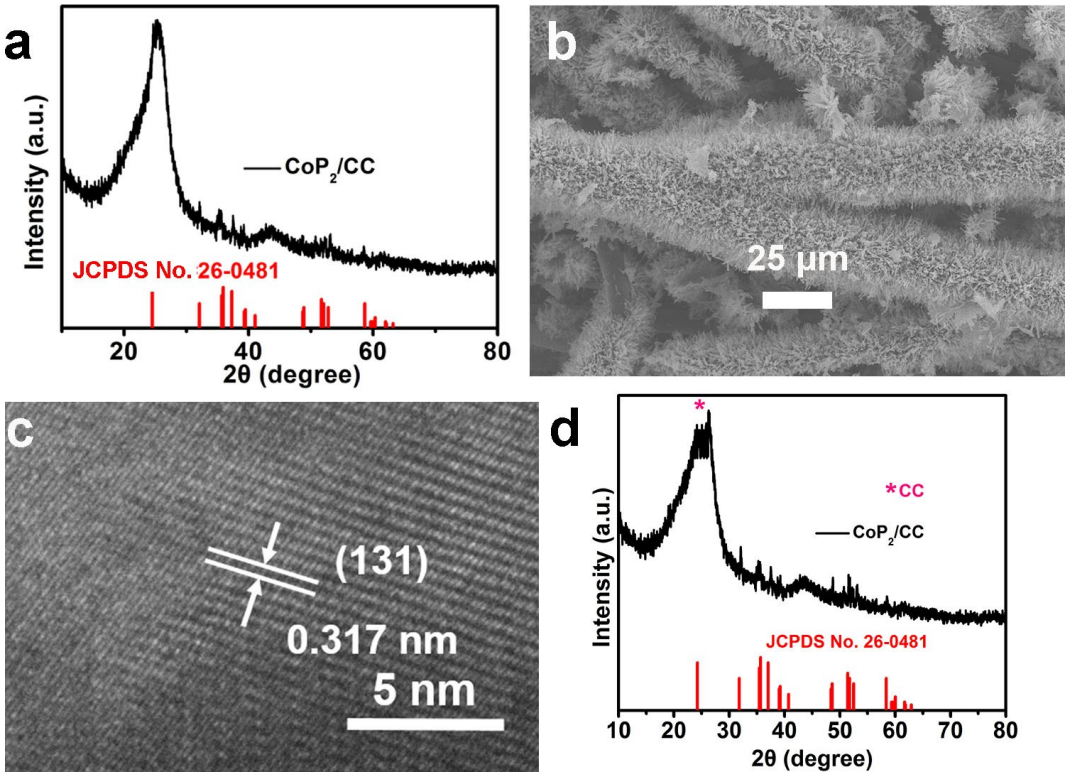

Fig. S4. (a) XRD pattern for CoP_2/CC. (b) SEM image for CoP_2/CC. (c) HRTEM image for CoP_2. (d) XRD pattern for CoP_2/CC after long-term NRR electrolysis.

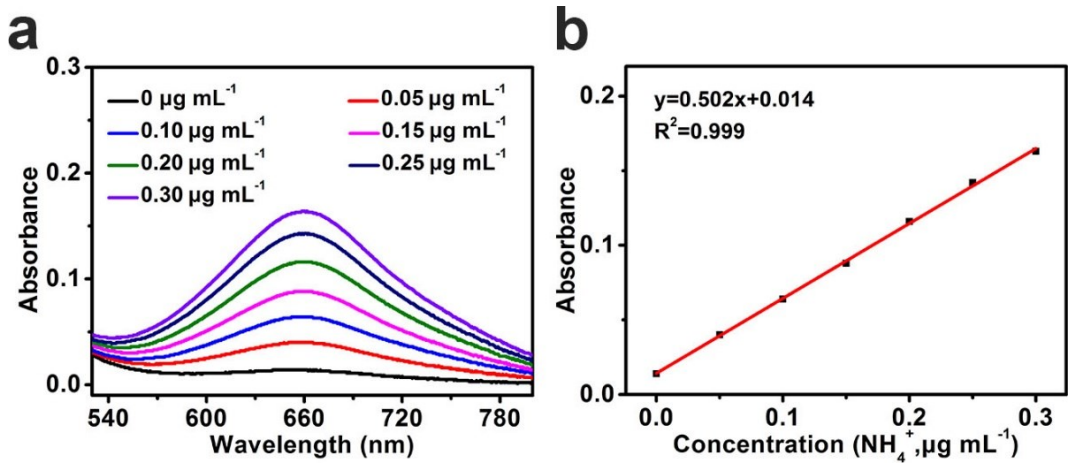

Fig. S5. (a) UV-Vis absorption spectra of indophenol assays with NH_4^+ ions after incubated for 2 h at room temperature. (b) Calibration curve used for estimation of NH_4^+.

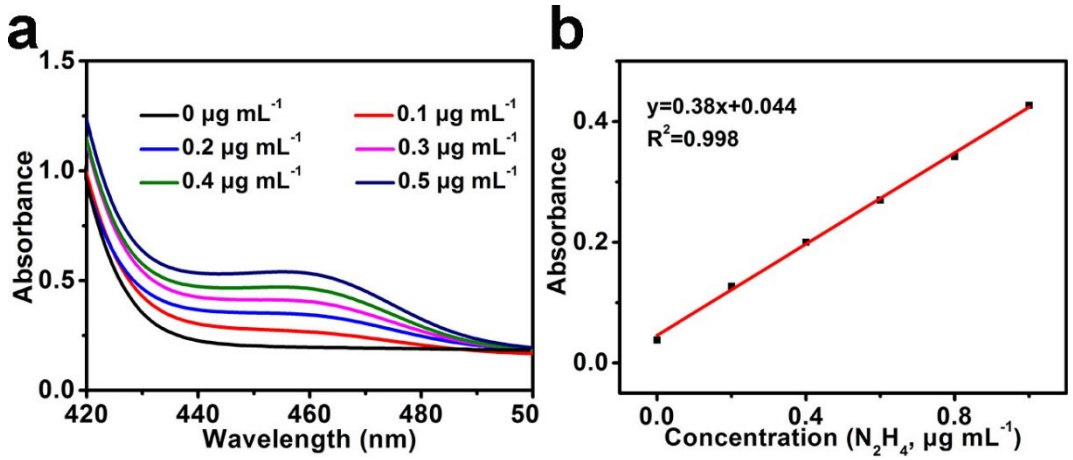

Fig. S6. (a) UV-Vis absorption spectra of various N_2H_4 concentrations after adding into chemical indicator by the method of Watt. (b) Calibration curve used for calculatin of N_2H_4 concentrations.

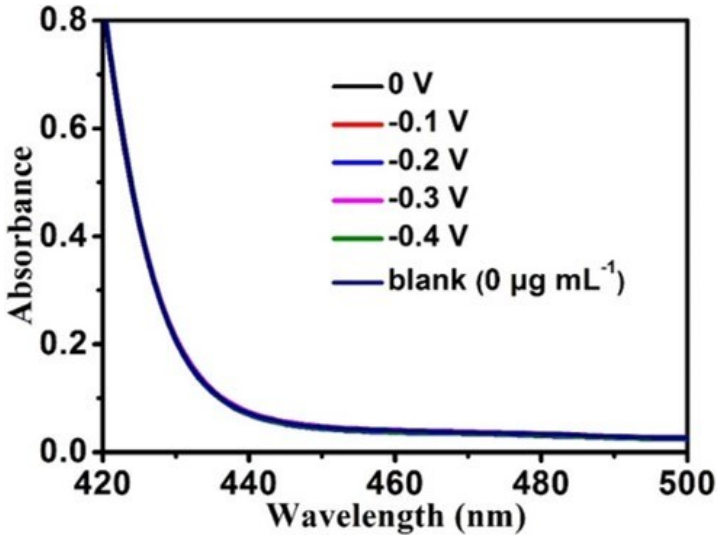

Fig. S7. UV-Vis absorption spectra of the electrolytes estimated by the method of Watt and Chrisp before and after 2 h electrolysis in N2 atmosphere at each given potential at ambient conditions using CoP_3/CC as the working electrode.

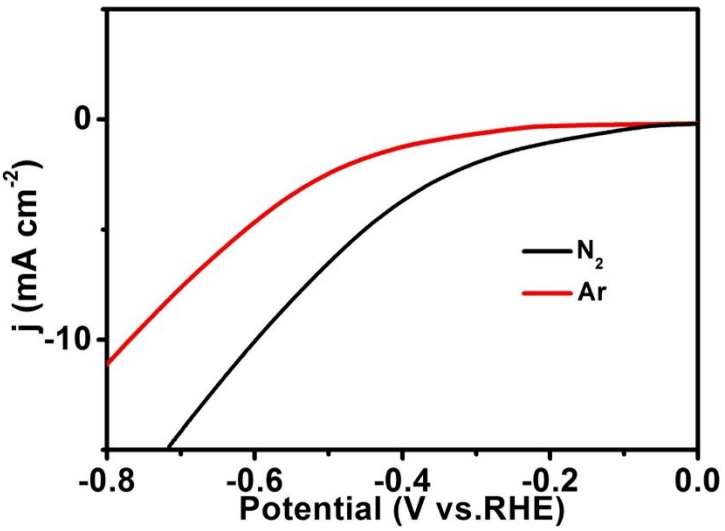

Fig. S8. LSV curves of CoP_3/CC in Ar-and N_2-saturated 0.1 M Na_2SO_4 at a scan rate of 5 mV s^{-1}.

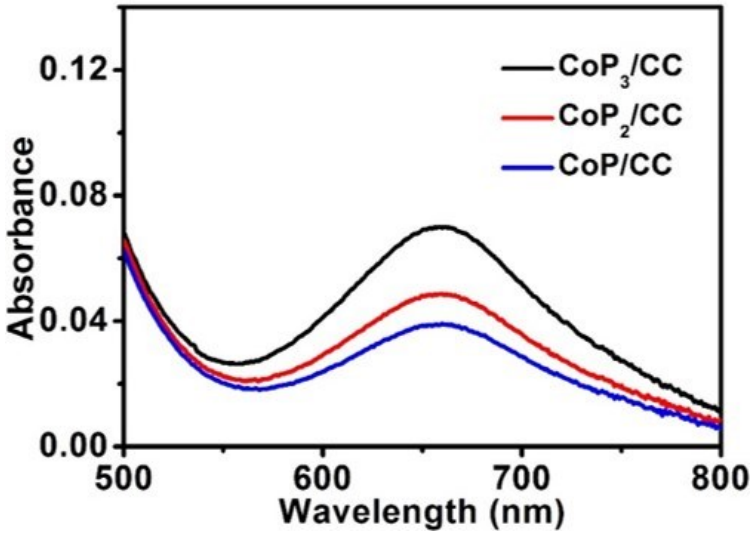

Fig. S9. UV-Vis absorption spectra of the electrolyte stained with indophenol indicator after charging at –0.20 V for 2 h under different electrode conditions.

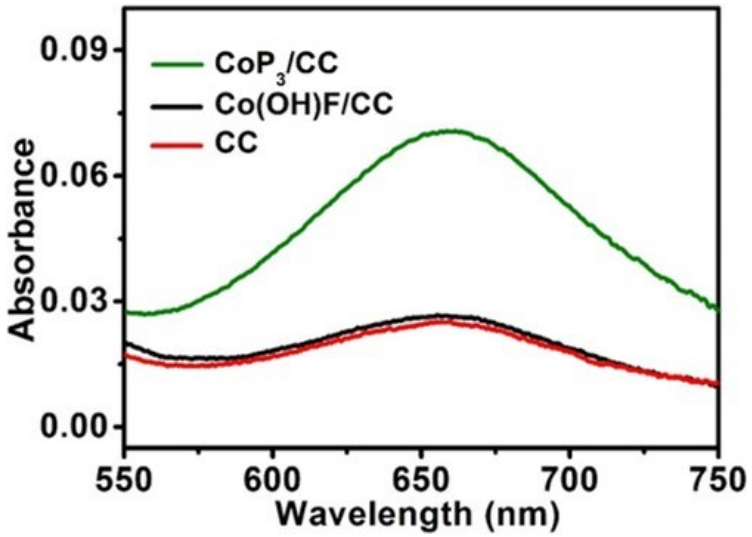

Fig. S10. UV-Vis absorption spectra of the electrolyte stained with indophenol indicator after charging at –0.20 V for 2 h under different electrode conditions.

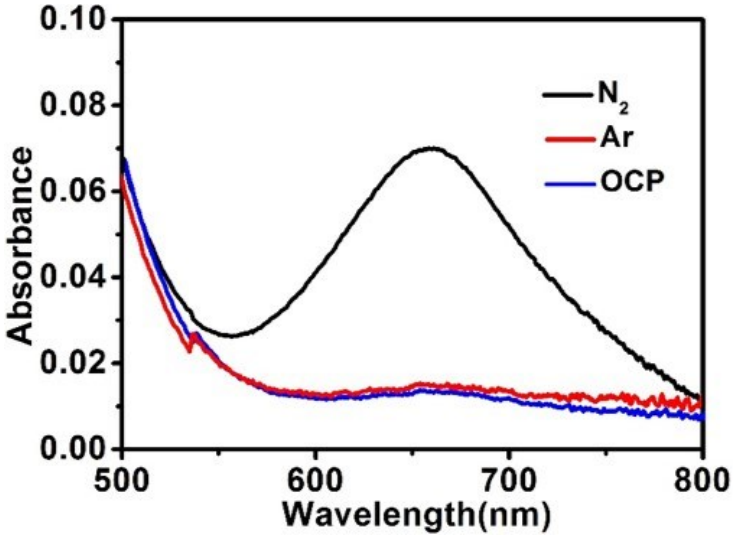

Fig. S11. UV-Vis absorption spectra of the electrolyte stained with indophenol indicator after charging at –0.20 V for 2 h under different electrochemical conditions.

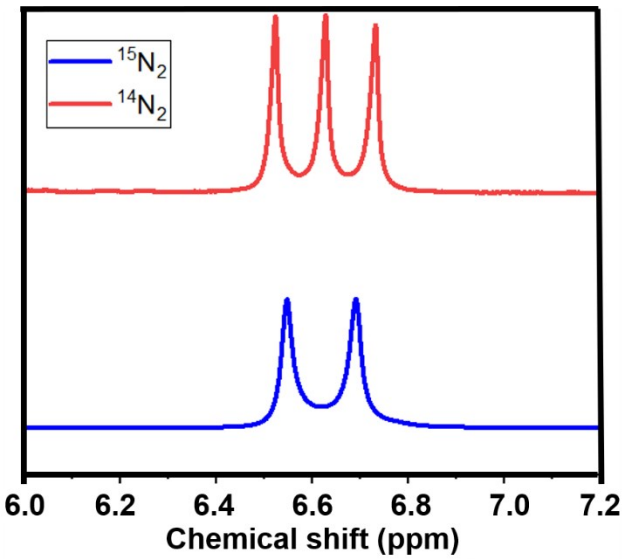

Fig. S12. ^{15}N isotope labeling experiment. ^{1}H NMR spectra for the post-electrolysis 0.1 M Na_2SO_4 electrolytes with $^{15}N_2$ and $^{14}N_2$ as the feeding gas.

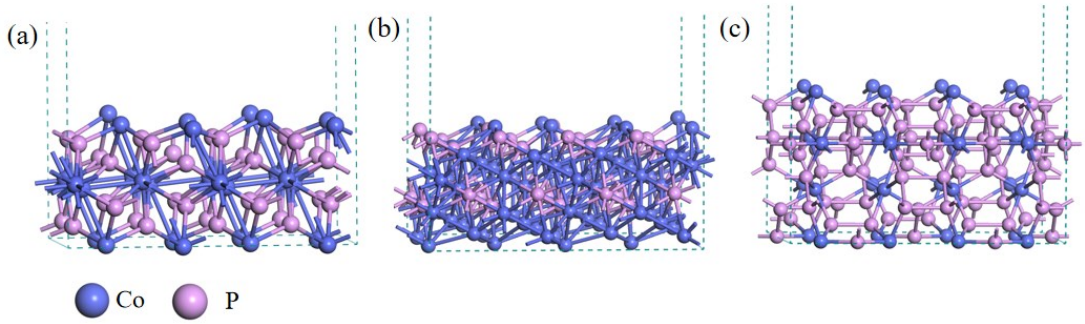

Fig. S13. Surface structures of (a) CoP, (b) CoP_2, (c) CoP_3.

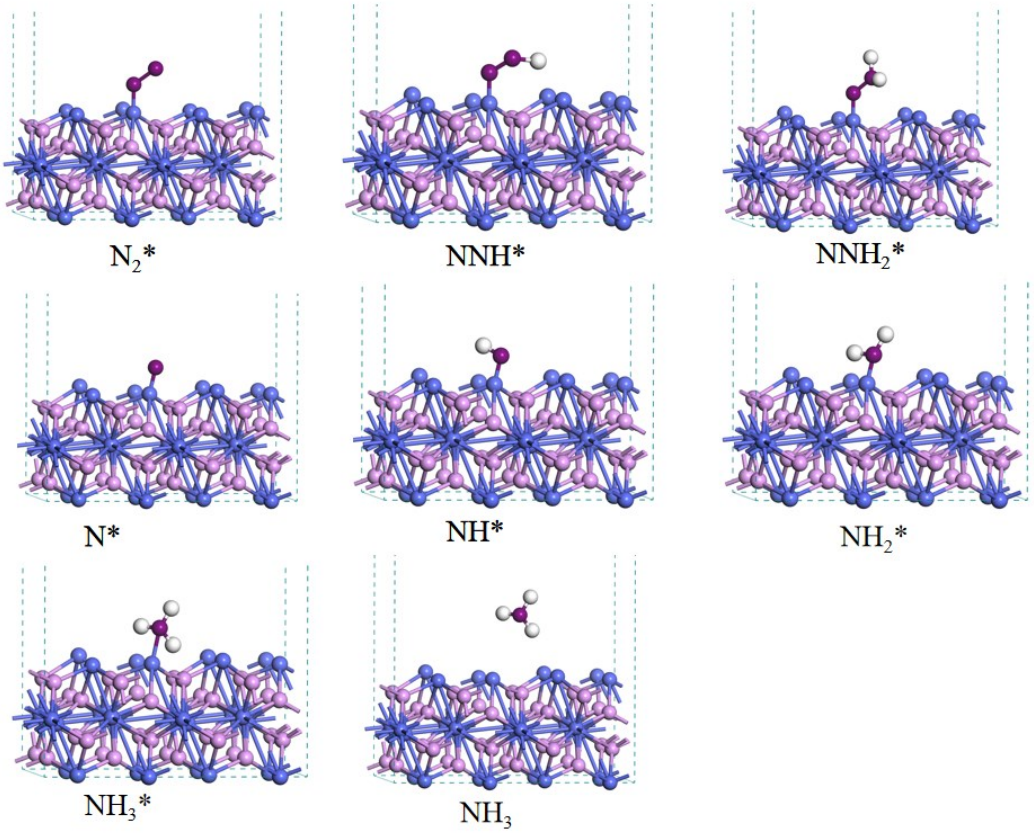

Fig. S14. The corresponding structure diagram of N_2 reduced to NH_3 on the surface of CoP (N_2-NNH, NNH_2, N, NH, NH_2, NH_3).

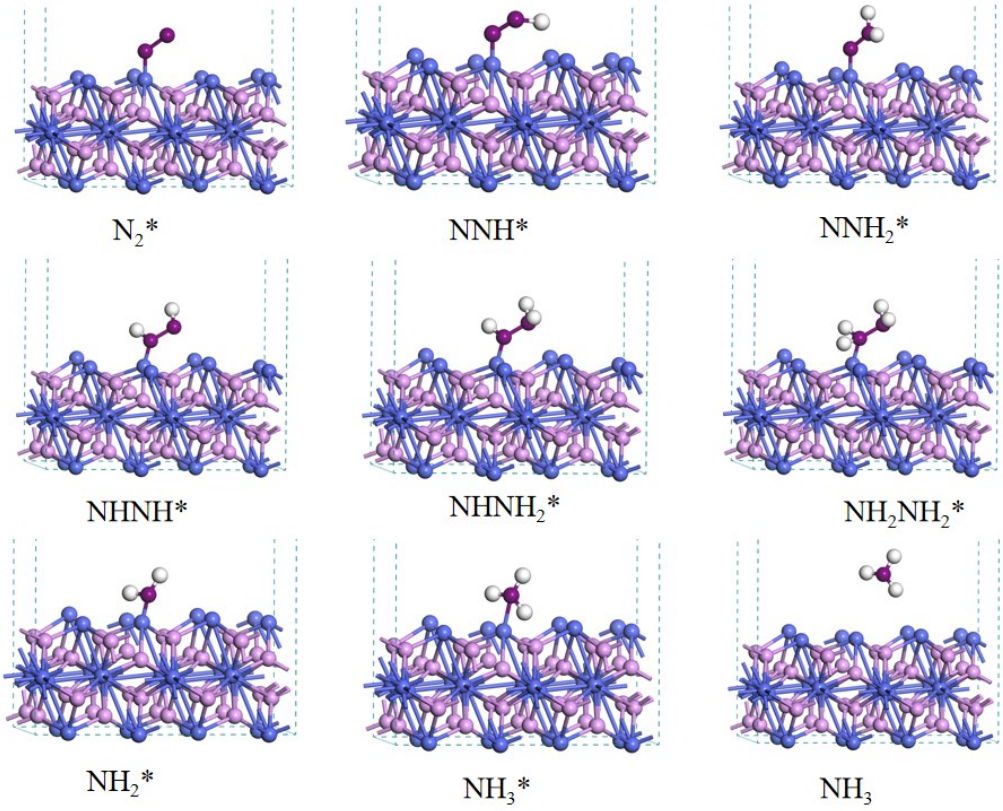

Fig. S15. The corresponding structure diagram of N_2 reduced to NH_3 on the surface of CoP (N_2-NNH, NHNH, $NHNH_2$, NH_2NH_2, NH_2, NH_3).

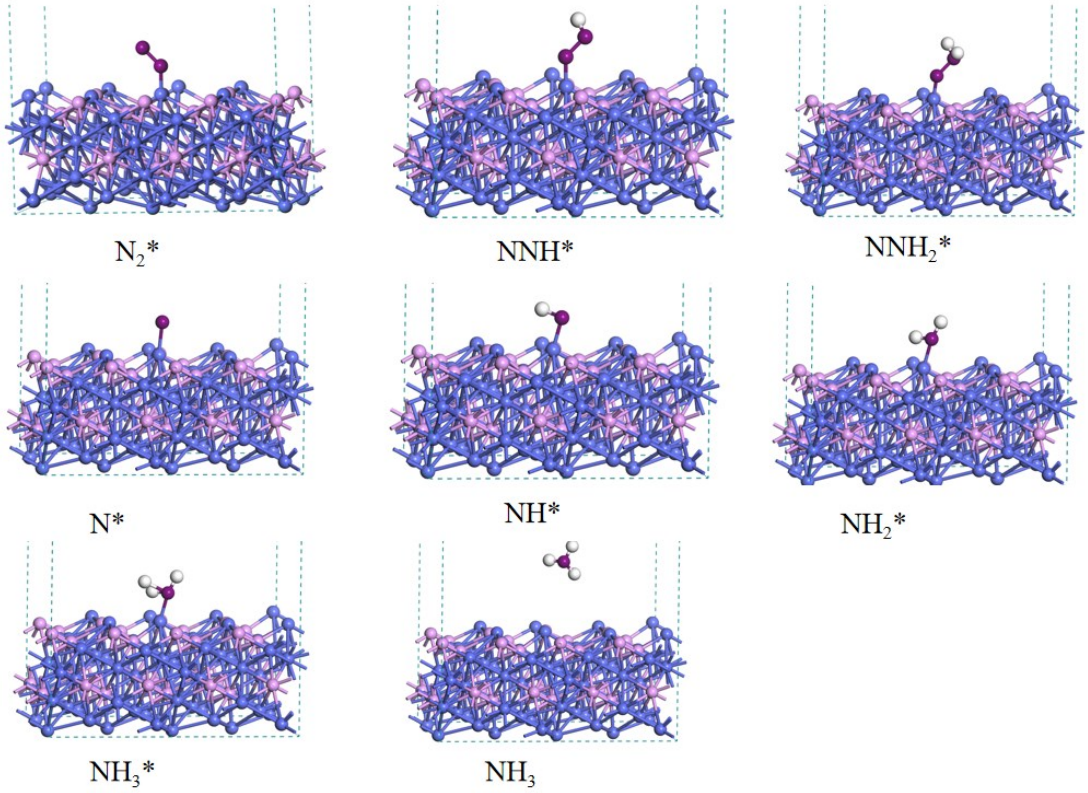

Fig. S16. The corresponding structure diagram of N_2 reduced to NH_3 on the surface of CoP_2 (N_2-NNH, NNH_2, N, NH, NH_2, NH_3).

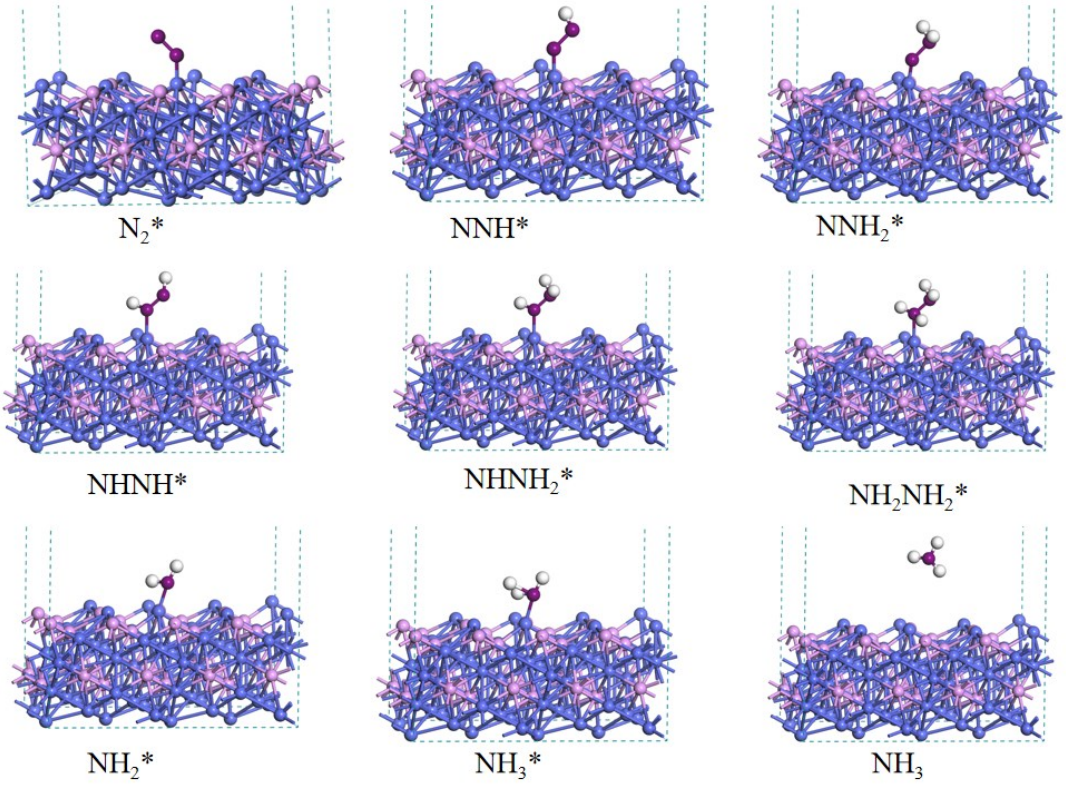

Fig. S17. The corresponding structure diagram of N_2 reduced to NH_3 on the surface of CoP_2 (N_2-NNH, NHNH, $NHNH_2$, NH_2NH_2, NH_2, NH_3).

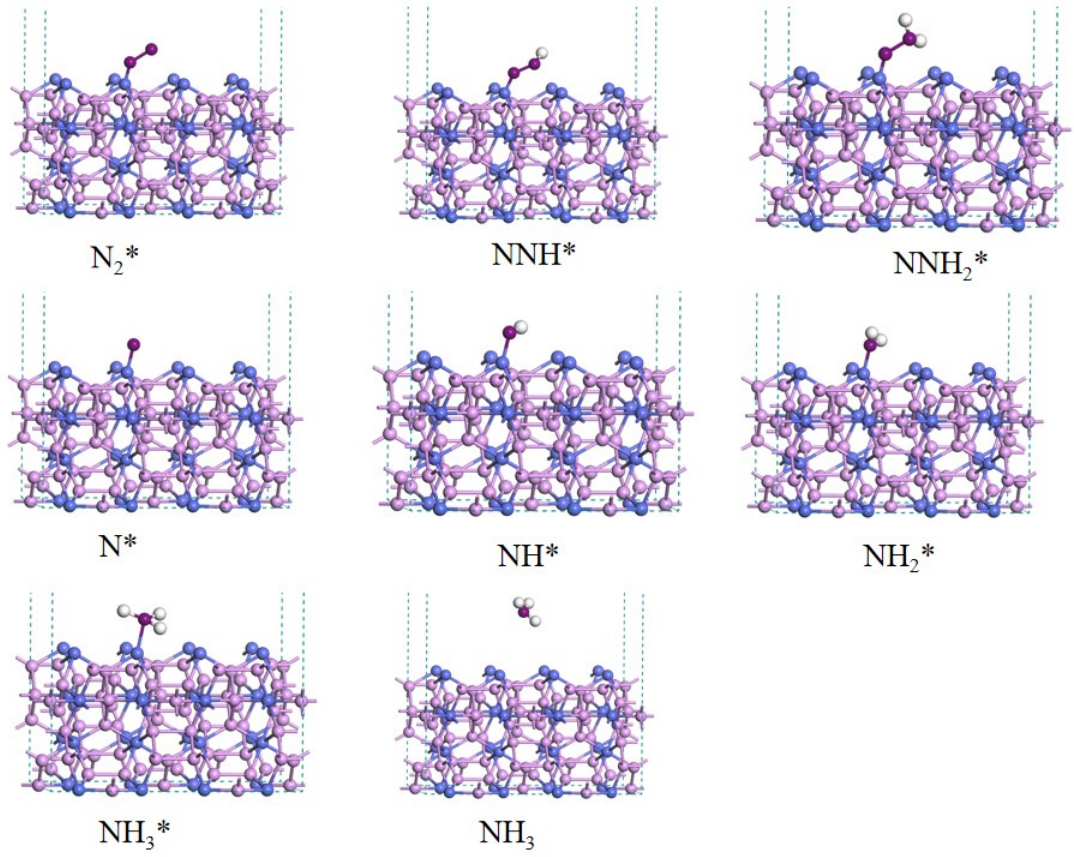

Fig. S18. The corresponding structure diagram of N_2 reduced to NH_3 on the surface of CoP_3 (N_2-NNH, NNH_2, N, NH, NH_2, NH_3).

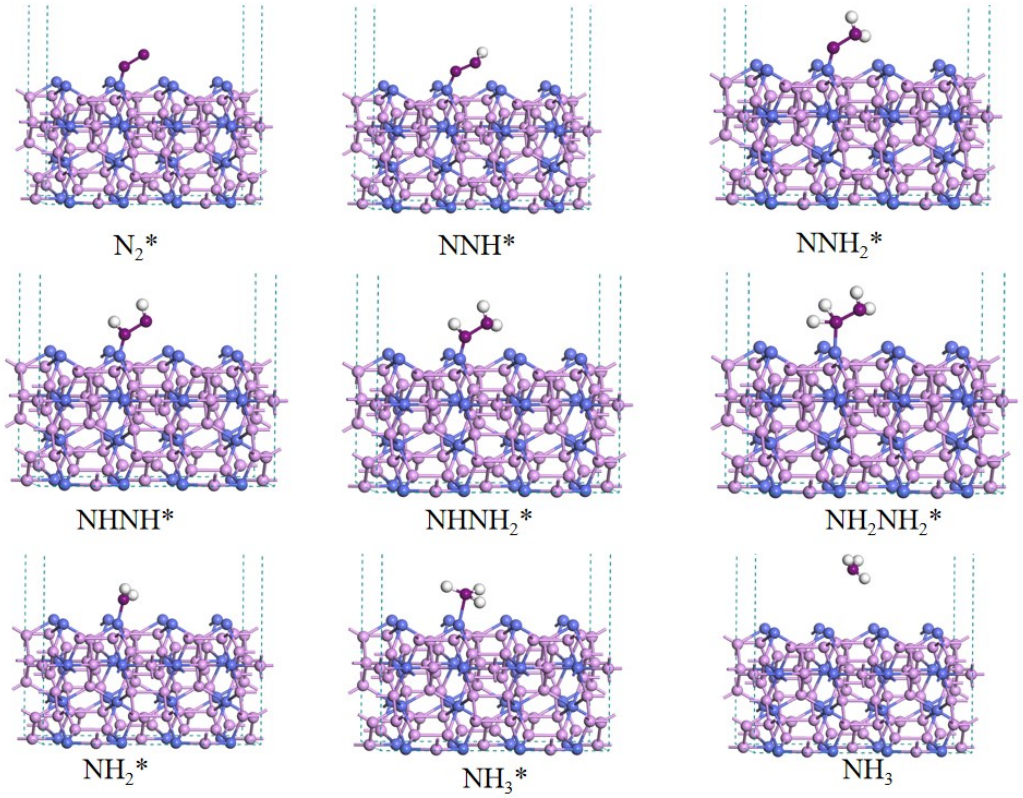

Fig. S19. The corresponding structure diagram of N_2 reduced to NH_3 on the surface of CoP_3 (N_2-NNH, NHNH, $NHNH_2$, NH_2NH_2, NH_2, NH_3).

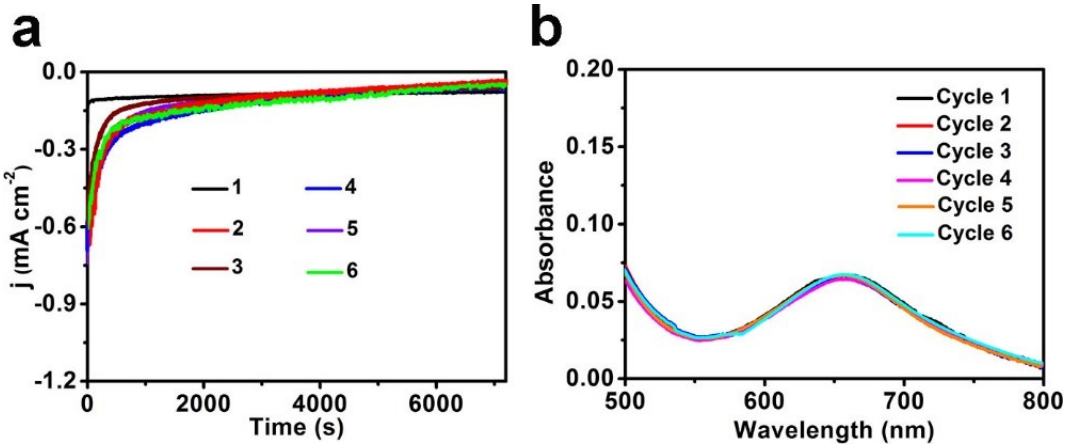

Fig. S20. (a) Time-dependent current density curves of CoP_3/CC in 0.1 M Na_2SO_4 N_2-saturated solution at –0.2 V *vs*. RHE. (b) UV-Vis absorption spectra of the electrolytes stained with indophenol indicator after NRR electrolysis for 2 h.

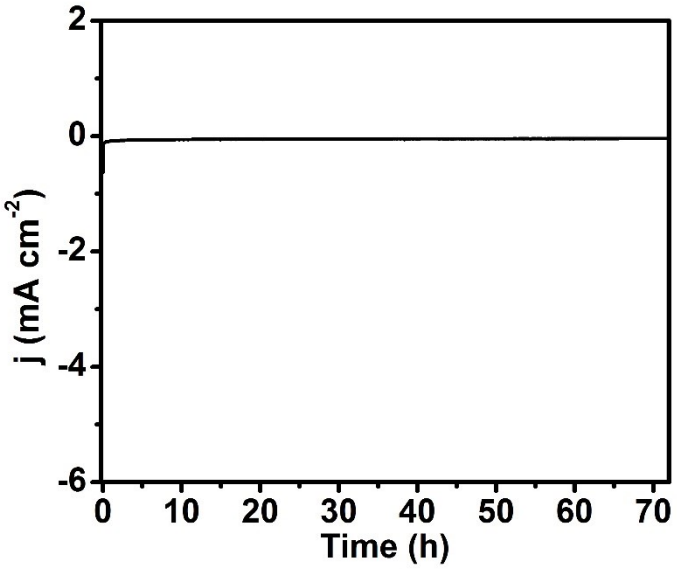

Fig. S21. Time-dependent current density curve at potential of –0.2 V using CoP_3/CC catalyst for 72 h.

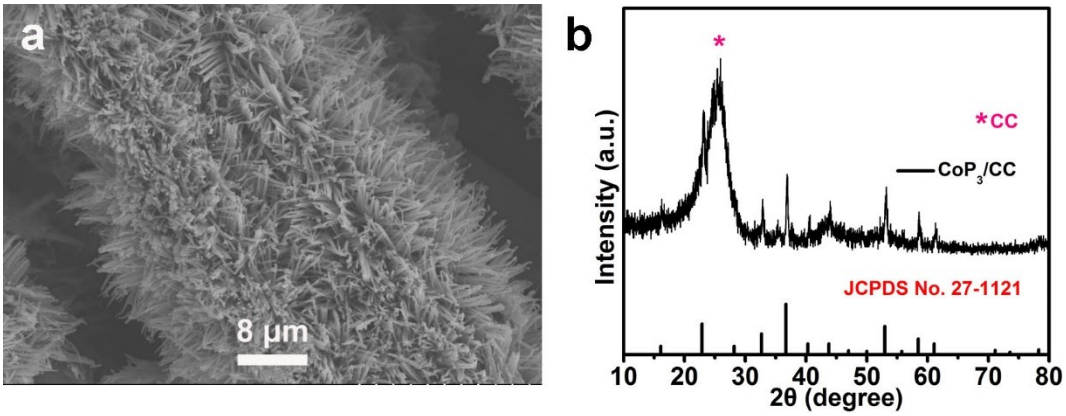

Fig. S22. (a) SEM image of CoP_3/CC after long-term electrocatalysis in 0.1 M Na_2SO_4. (b) XRD pattern for CoP_3/CC after long-term NRR electrolysis.

Table S1. Comparison of the electrocatalytic NRR performance of CoP_3/CC with other catalysts.

Catalyst	Electrolyte	NH_3 yield	FE (%)	Ref.
CoP_3/CC	**0.1 M Na_2SO_4**	**3.61×10^{-11} mol s^{-1} cm^{-2}**	**11.94**	**This work**
CoP HNC	1.0 M KOH	10.78 μg h^{-1} mg^{-1}_{cat}	7.36	1
CoP/CNs	0.1 M Na_2SO_4	48.9 μg h^{-1} mg^{-1}_{cat}	8.7	2
MoS_2/CC	0.1 M Na_2SO_4	8.08×10^{-11} mol s^{-1} cm^{-2}	1.17	3
Boron-doped graphene	0.5 M Na_2SO_4	9.8 μg h^{-1} mg^{-1}_{cat}	10.8	4
Fe_2O_3 nanorods	0.1 M Na_2SO_4	15.9 μg h^{-1} mg^{-1}_{cat}	0.94	5
B_4C	0.1 M HCl	26.57 μg h^{-1} mg^{-1}_{cat}	15.95	6
VN	0.1 M HCl	2.48×10^{-10} mol s^{-1} cm^{-2}	3.58	7
Fe_2O_3-CNT	$KHCO_3$	0.22 μg h^{-1} cm^{-2}	0.15	8
Au-Fe_3O_4	0.1 M Na_2SO_4	21.42 μg h^{-1} mg^{-1}_{cat}	10.54	9
TiO_2/Ti	0.1 M Na_2SO_4	9.16×10^{-11} mol h^{-1} cm^{-2}	2.5	10
Mo nanofilm	0.1 M Na_2SO_4	1.89 μg h^{-1} cm^{-2}	0.72	11
Fe_3C@C	0.05 M Na_2SO_4	8.53 μg h^{-1} mg^{-1}_{cat}	9.15	12
Cu/PI	0.1 M KOH	12.4 μg h^{-1} cm^{-2}	6.56	13
B-TiO_2	0.1 M Na_2SO_4	14.4 μg h^{-1} mg^{-1}_{cat}	3.4	14
La_2O_3	0.1 M Na_2SO_4	17.04 μg h^{-1} mg^{-1}_{cat}	4.76	15
Au nanorods	0.1 M KOH	1.648 μg h^{-1} cm^{-2}	4	16
S-CNS	0.1 M Na_2SO_4	19.07 μg h^{-1} mg^{-1}_{cat}	7.47	17
TiS_2	0.1 M Na_2SO_4	16.02 μg h^{-1} mg^{-1}_{cat}	5.50	18
C-TiO_2	0.1 M Na_2SO_4	16.22 μg h^{-1} mg^{-1}_{cat}	1.84	19
TiO_2-rGO	0.1 M Na_2SO_4	15.13 μg h^{-1} mg^{-1}_{cat}	3.3	20
$Pd_{0.2}Cu_{0.8}$/rGO	0.1 M KOH	2.80 μg h^{-1} mg^{-1}_{cat}	4.5	21
Bi_2MoO_6	0.1 M HCl	20.46 μg h^{-1} mg^{-1}_{cat}	8.17	22
N-doped porous carbon	0.05 M Na_2SO_4	23.8 μg h^{-1} mg^{-1}_{cat}	1.42	23

References

1 W. Guo, Z. Liang, J. Zhao, B. Zhao, B. Zhu, K. Cai, R. Zou and Q. Xu, *Small Methods*, 2018, **2**, 1800204.

2 S. Zhang, W. Gong, Y. Lv, H. Wang, M. Han, G. Wang, T. Shi and H. Zhang, *Chem. Commun*., 2019, **55**, 12376–12379.

3 L. Zhang, X. Ji, X. Ren, Y. Ma, X. Shi, Z. Tian, A. M. Asiri, L. Chen, B. Tang and X. Sun, *Adv. Mater*., 2018, **30**, 1800191.

4 X. Yu, P. Han, Z. Wei, L. Huang, Z. Gu, S. Peng, J. Ma and G. Zheng, *Joule*, 2018, **2**, 1610–1622.

5 X. Xiang, Z. Wang, X. Shi, M. Fan and X. Sun, *ChemCatChem*, 2018, **10**, 4530–4535.

6 W. Qiu, X. Xie, J. Qiu, W. Fang, R. Liang, X. Ren, X. Ji, G. Cui, A. M. Arisi, G. Cui, B. Tang and X. Sun, *Nat. Commun*., 2018, **9**, 3485.

7 X. Zhang, R. Kong, H. Du, L. Xia and F. Qu, *Chem. Commun.*, 2018, **54**, 5323–5325.

8 S. Chen, S. Perathoner, C. Ampelli, C. Mebrahtu, D. Su, G. Centi, *Angew. Chem., Int. Ed*., 2017, **56**, 2699–2703.

9 J. Zhang, Y. Ji, P. Wang, Q. Shao, Y. Li and X. Huang, *Adv. Funct. Mater*., 2019, **8**, 1906579.

10 R. Zhang, X. Ren, X. Shi, F. Xie, B. Zheng, X. Guo and X. Sun, *ACS Appl. Mater. Interfaces*, 2018, **10**, 28251–28255.

11 D. Yang, T. Chen and Z. Wang, *J. Mater. Chem. A*, 2017, **5**, 18967–18971.

12 M. Peng, Y. Qiao, M. Luo, M. Wang, S. Chu, Y. Zhao, P. Liu, J. Liu and Y. Tan, *ACS Appl. Mater. Interfaces*, 2019, **11**, 40062–40068.

13 Y. Lin, S. Zhang, Z. Xue, J. Zhang, H. Su, T. Zhao, G. Zhai, X. Li, M. Antonietti and J. Chen, *Nat. Commun*., 2019, **10**, 4380.

14 Y. Wang, K. Jun, Q. Pan, Y. Xu, Q. Liu, G. Cui, X. Guo and X. Sun, *ACS Sustainable Chem. Eng*., 2019, **7**, 117–122.

15 B. Xu, Z. Liu, W. Qiu, Q. Liu, X. Sun, G. Cui, Y. Wu and X. Xiong, *Electrochim. Acta*., 2018, **298**,106–111.

16 D. Bao, Q. Zhang, F. Meng, H. Zhong, M. Shi, Y. Zhang, J. Yan, Q. Jiang and X. Zhang, *Adv. Mater*., 2017, **29**, 1604799.

17 L. Xia, X. Wu, Y. Wang, Z. Niu, Q. Liu, T. Li, X. Shi, A. M. Arisi and X. Sun, *Small Methods*, 2018, **6**, 1800251.

18 K. Jia, Y. Wang, L. Qiu, J. Gao, Q. Pan, W. Kong, X. Zhang, A. A. Alzahrani, K. A. Alzahrani, B.Zhong, X. Guo and L. Yang, *Inorg. Chem. Front*., 2019, DOI: 10.1039/C91I00301K.

19 K. Jia, Y. Wang, Q. Pan, B. Zhong, Y. Luo, G. Cui, X. Guo and X. Sun, *Nanoscale*, 2019, **1**, 961–964

20 X. Zhang, Q. Liu, X. Shi, A. M. Arisi, Y. Luo, X. Sun, T. Li, *J. Mater. Chem. A*, 2018, **6**, 17303–17306.

21 M. Shi, D. Bao, S. Li, B. Wulan, J. Yan and Q. Jiang, *Adv. Energy Mater.*, 2018, **8**, 1800124.

22 Z. Xing, W. Kong, T. Wu, H. Xie, T. Wang, Y. Luo, X. Shi, A. M. Asiri, Y. Zhang and X. Sun, *ACS Sustainable Chem. Eng*., 2019, **7**, 12692–12696.

23 Y. Liu, Y. Su, X. Quan, X. Fan, S. Chen, H. Yu, H. Zhao, Y. Zhang and J. Zhao, *ACS Catal*., 2018, **8**, 1186–1191.